

Electronic Supplementary Information

Self-Assembled via Axial Coordination Cobalt(II)porphyrin-Fulleropyrrolidine Triad with Photoinduced Electron Transfer

N.G. Bichan,[®] E.N. Ovchenkova, N.O. Kudryakova, A.A. Ksenofontov, M.S. Gruzdev, T.N. Lomova

G.A. Krestov Institute of Solution Chemistry of the Russian Academy of Sciences, Ivanovo,
153045 Russia.

E-mail: bng@isc-ras.ru

	Page
Figure S1. UV-vis spectra of PyC ₆₀ in toluene at 298 K. $C_{\text{PyC}_{60}} = 3.60 \times 10^{-5}$ (1), 4.85×10^{-5} (2), 6.04×10^{-5} (3), 9.19×10^{-5} (4), 9.98×10^{-5} (5), 1.20×10^{-4} (6), 1.62×10^{-4} (7) M	2
Figure S2. Plots of $\lg I$ vs $\lg C_{\text{PyC}_{60}}$ for the reaction of PyC ₆₀ with Co ^{II} P at $\tau = 0$.	2
Figure S3. Plot of $\lg k_{\text{ef}}$ versus $\lg C_{\text{PyC}_{60}}$ for the reaction of Co ^{II} P with PyC ₆₀ in toluene at 298 K.	2
Figure S4. IR spectrum of (PyC ₆₀) ₂ Co ^{II} P.	3
Figure S5. ¹ H NMR spectra of compounds Co ^{II} P (a), (PyC ₆₀) ₂ Co ^{II} P (b) and PyC ₆₀ (c) in CDCl ₃ .	3
Synthesis of (2,3,7,8,12,18-hexamethyl,13,17-diethyl,5-(2-pyridyl)porphinato)cobalt(II)	4
Synthesis of 1'-N-methyl-2'-(pyridin-4-yl)pyrrolidino[3',4':1,2][60]fullerene	4
Figure S6. MALDI TOF mass-spectra of the PyC ₆₀	5
Table S1. The basic structural parameters (bond lengths, angles, Mulliken atomic charges (q)) of the (PyC ₆₀) ₂ Co ^{II} P optimized structure (B3LYP-D3/6-31G (d,p)).	6
Figure S7. TDDFT spectrum of the PyC ₆₀ (B3LYP-D3/6-31G (d,p), PCM(toluene)).	7
Table S2. Theoretically calculated spectral characteristics of of the PyC ₆₀ in toluene and corresponding oscillator strengths (f) (B3LYP-D3/6-31G (d,p)).	7
Table S3. The photocurrent density of system Ti film 0.5 M Na ₂ SO ₄ Pt.	8
Figure S8. Cyclic voltammogram of the PyC ₆₀ (a), Co ^{II} P (b) and (PyC ₆₀) ₂ Co ^{II} P (c). Scan rate: 100 mV s ⁻¹ .	8
Table S4. Redox potentials, free-energy changes for charge separation (ΔG_{CS}) and recombination (ΔG_{CR}) for the (PyC ₆₀) ₂ Co ^{II} P in CH ₂ Cl ₂ .	9

Figure S1. UV-vis spectra of PyC₆₀ in toluene at 298 K. $C_{\text{PyC}_{60}} = 3.60 \times 10^{-5}$ (1), 4.85×10^{-5} (2), 6.04×10^{-5} (3), 9.19×10^{-5} (4), 9.98×10^{-5} (5), 1.20×10^{-4} (6), 1.62×10^{-4} (7) M.

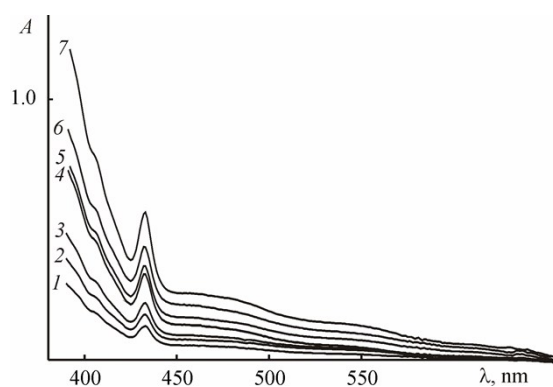


Figure S2. Plots of $\lg I$ vs $\lg C_{\text{PyC}_{60}}$ for the reaction of PyC₆₀ with Co^{II}P at $\tau = 0$.

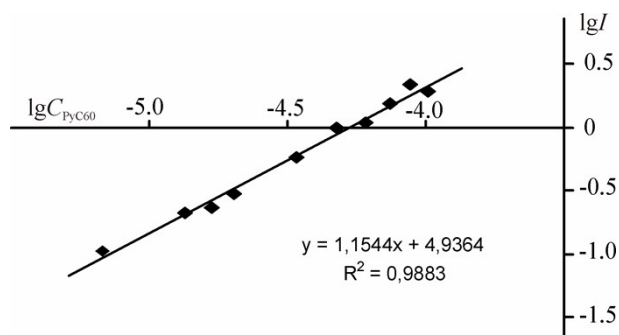


Figure S3. Plot of $\lg k_{\text{ef}}$ versus $\lg C_{\text{PyC}_{60}}$ for the reaction of Co^{II}P with PyC₆₀ in toluene at 298 K.

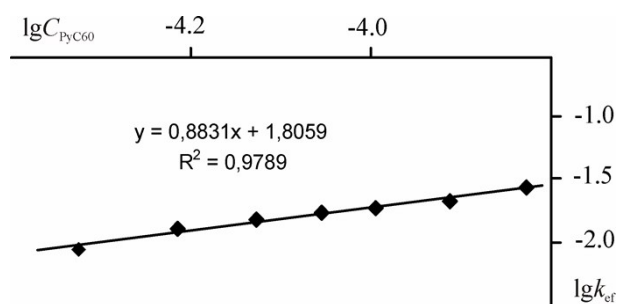


Figure S4. IR spectrum of $(\text{PyC}_{60})_2\text{Co}^{\text{II}}\text{P}$.

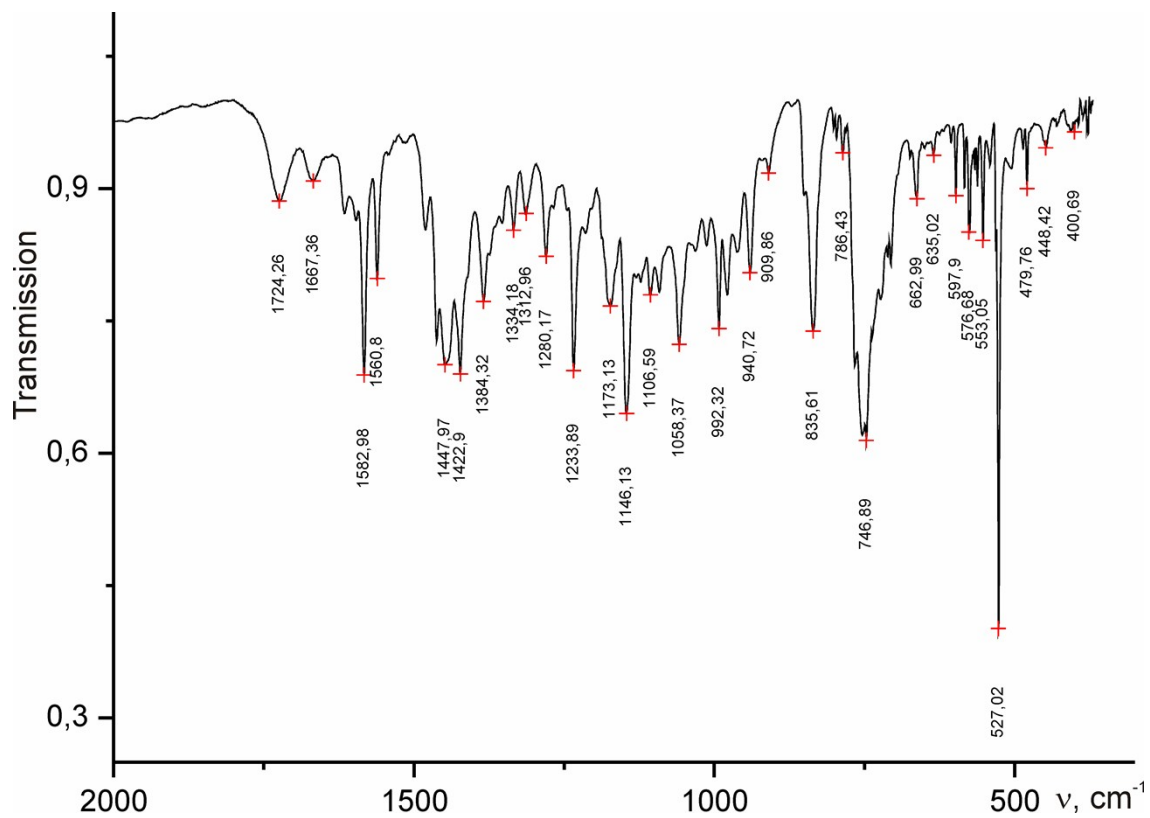
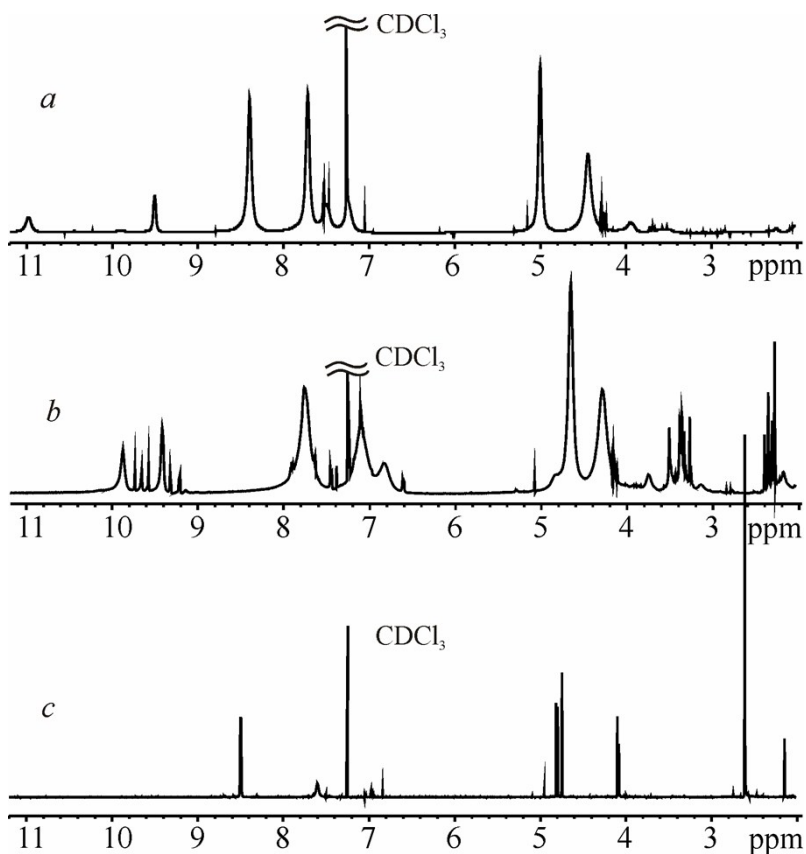


Fig. S5. ^1H NMR spectra of compounds $\text{Co}^{\text{II}}\text{P}$ (a), $(\text{PyC}_{60})_2\text{Co}^{\text{II}}\text{P}$ (b) and PyC_{60} (c) in CDCl_3 .



Synthesis of (2,3,7,8,12,18-hexamethyl,13,17-diethyl,5-(2-pyridyl)porphinato)cobalt(II), Co^{II}P

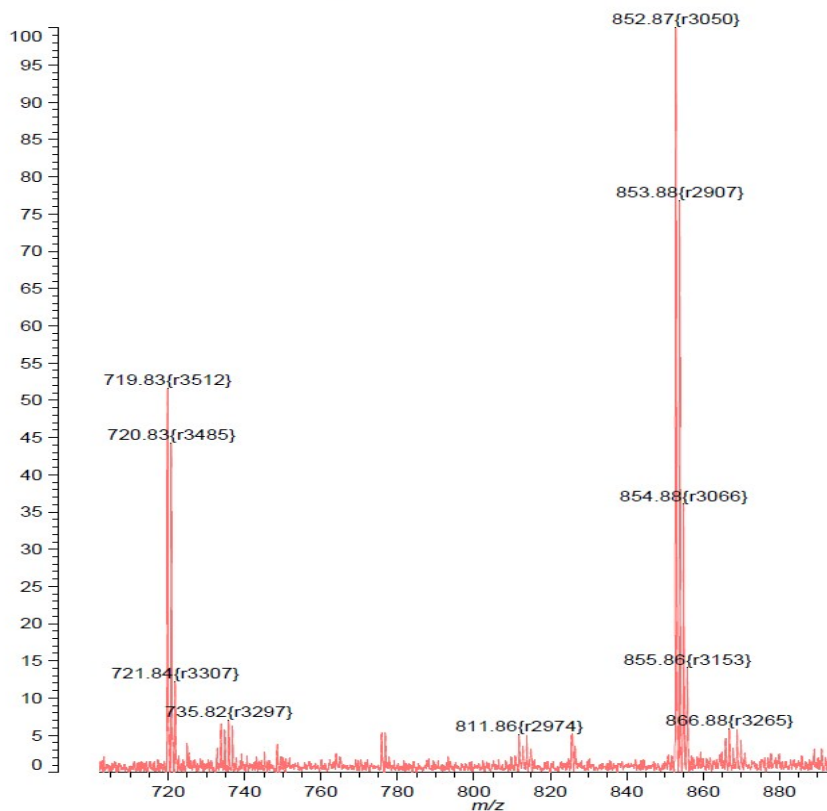
Co(AcO)₂·4H₂O (47.0 mg, 0.19 mmol) and (2,3,7,8,12,18-hexamethyl,13,17-diethyl,5-(2-pyridyl)porphyrin H₂P (20.0 mg, 0.04 mmol) were reacted in boiling dimethylformamide (10 ml) for 40-50 min. Completion of the reaction was monitored by TLC, until no traces of starting material were detected. The reaction mixture was cooled, after dilution with water the products were extracted into chloroform and purified by flash chromatography (Al₂O₃/CHCl₃). The red zone display on the chromatogram corresponding to Co^{II}P.

Synthesis of 1'-N-methyl-2'-(pyridin-4-yl)pyrrolidino[3',4':1,2][60]fullerene, PyC₆₀

A solution of 100 mg (0.14 mmol) of C₆₀, 80 mg (0.70 mmol) of pyridine-4-carboxaldehyde and 43 mg (0.48 mmol) of N-methylglycine in 90 ml of toluene was stirred at reflux temperature for 2 h. Then the solvent was removed in vacuo. The formation of PyC₆₀ was monitored by TLC and UV-Vis of the reaction mixture by the appearance of absorption with $\lambda_{\max} = 433$ nm [M. Prato, M. Maggini, C. Giacometti, G.Scorrano et al. *Tetrahedron*, 1996, **52**, 5221; P.A. Troshin, S.I. Troyanov, G.N. Boiko, R.N. Lyubovskaya et al. *Fullerenes, nanotubes, and carbon nanostructures*, 2004, **12**, 413]. The reaction mixture was purified by column chromatography on Al₂O₃ (elution with the mixture of toluene- ethyl acetate (20:1)). Yield: 0.64 mg (52%).

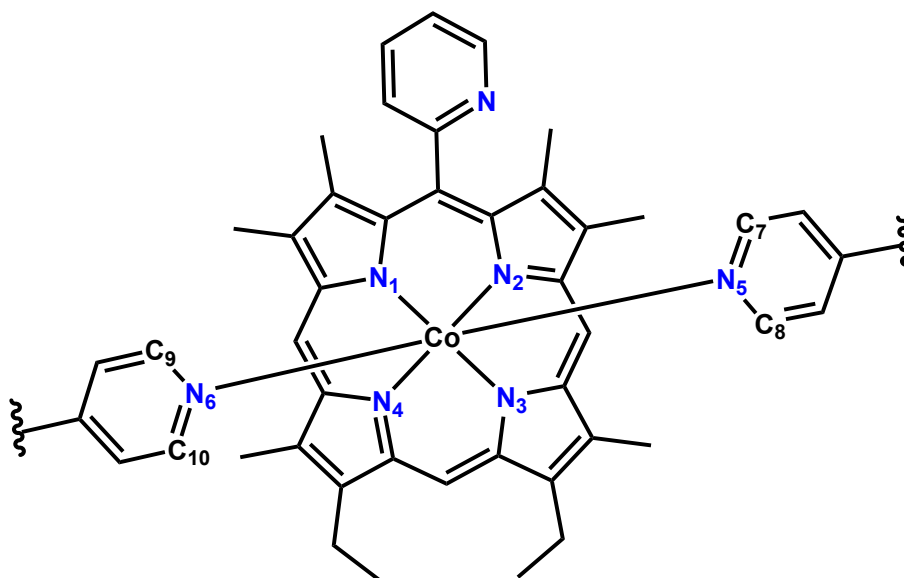
Figure S6. MALDI TOF mass-spectra of the PyC₆₀.

Shimadzu Biotech Axima Confidence 2.9.3.20110624: Mode Reflectron, Power: 50, Blanked, %Int. 103 mV[sum= 11715 mV] Profiles 1-114 Smooth Av 5 -Baseline 20



Although the PyC₆₀ is expected to give one signal in MALDI TOF mass-spectrum with m/z corresponding to the formula C₆₈H₁₀N₂ (calc. m/z 854.0) it gives the signal with m/z 719.83, corresponding to the [C₆₀]⁺. It is expected that this signal are formed under the conditions of mass-spectrum registration.

Table S1. The basic structural parameters (bond lengths, angles, NBO atomic charges (q)) of the $(\text{PyC}_{60})_2\text{Co}^{\text{II}}\text{P}$ optimized structure (B3LYP-D3/6-31G (d,p)).



	Bond length, Å		Angle, grad		q , e^-
Co–N(1)	2.043	N(1)–Co–N(2)	89.98	Co	1.299
Co–N(2)	2.060	N(2)–Co–N(3)	91.23	N(1)	-0.637
Co–N(3)	2.094	N(3)–Co–N(4)	89.50	N(2)	-0.644
Co–N(4)	2.084	N(4)–Co–N(1)	91.27	N(3)	-0.640
Co–N(5)	2.288	N(1)–Co–N(3)	178.38	N(4)	-0.639
Co–N(6)	2.263	N(2)–Co–N(4)	178.48	N(5)	-0.497
		N(1)–Co–N(5)	91.55	N(6)	-0.491
		N(2)–Co–N(5)	88.45		
		N(3)–Co–N(5)	89.57		
		N(4)–Co–N(5)	91.99		
		Co–N(5)–C(7)	114.63		
		Co–N(5)–C(8)	118.83		
		N(1)–Co–N(6)	87.48		
		N(2)–Co–N(6)	91.02		
		N(3)–Co–N(6)	91.41		
		N(4)–Co–N(6)	88.17		
		Co–N(6)–C(9)	118.88		
		Co–N(6)–C(10)	120.10		

Figure S7. TDDFT spectrum of the PyC₆₀ (B3LYP-D3/6-31G (d,p), PCM(toluene)).

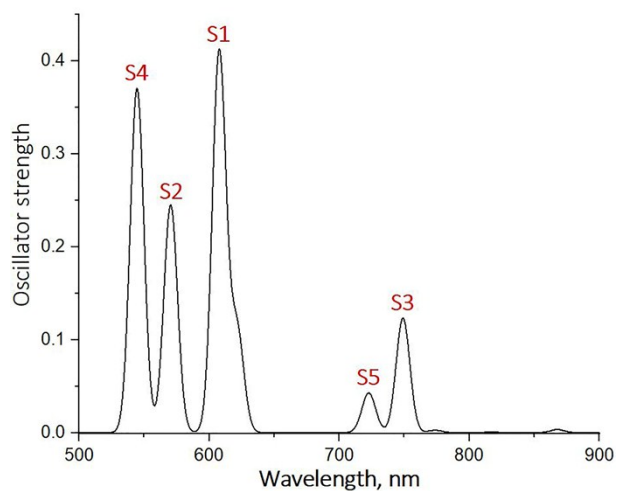


Table S2. Theoretically calculated spectral characteristics of the PyC₆₀ in toluene and corresponding oscillator strengths (*f*) (B3LYP-D3/6-31G (d,p)).

State	Transition	Energy, eV	<i>f</i>
S1	H-1 L	2.041	0.41
S2	H-1 L+8	2.174	0.25
S3	H-2 L	1.665	0.12
S4	H-3 L	2.278	0.23
S5	H-2 L+2	1.716	0.04

Table S3. The photocurrent density* of system Ti|film|0.5 M Na₂SO₄|Pt.

Titanium electrode with natural oxide film	j_{ph}^1 , $\mu\text{A cm}^{-2}$	j_{ph}^2 , $\mu\text{A cm}^{-2}$	j_{ph}^3 , $\mu\text{A cm}^{-2}$	j_{ph}^4 , $\mu\text{A cm}^{-2}$	j_{ph}^5 , $\mu\text{A cm}^{-2}$	j_{ph}^6 , $\mu\text{A cm}^{-2}$	j_{ph}^{avg} , $\mu\text{A cm}^{-2}$
NOF	0	0	0	0	0	0	0
Co ^{II} P ($C_{Co^{II}P} = 1.80 \times 10^{-5} \text{ M}$)	118.92	112.90	115.11	119.28	117.65	116.28	116.69
PyC ₆₀ ($C_{PyC60} = 1.47 \times 10^{-4} \text{ M}$)	95.19	97.71	96.35	99.13	95.13	95.12	96.58
(PyC ₆₀) ₂ Co ^{II} P ($C_{Co^{II}P} = 1.80 \times 10^{-5} \text{ M}$, $C_{PyC60} = 1.47 \times 10^{-4} \text{ M}$)	289.93	287.52	288.03	283.38	285.77	287.61	287.04

* $j_{ph} = i/S$, here i - photocurrent, μA ; S- the surface area of the modified electrode illuminated by monochromatic UV light (365 nm).

¹⁻⁶ - number of experiment

Figure S8. Cyclic voltammogram of the PyC₆₀ (a), Co^{II}P (b) and (PyC₆₀)₂Co^{II}P (c) in CH₂Cl₂ containig 0.1 M (n-Bu)₄NClO₄ supporting electrolyte. Scan rate: 100 mV s⁻¹.

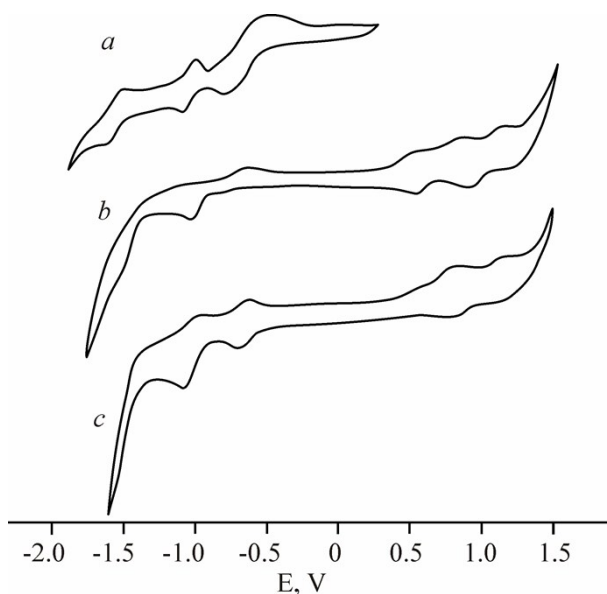


Table S4. Redox potentials, free-energy changes for charge separation (ΔG_{CS}) and recombination (ΔG_{CR}) for the $(\text{PyC}_{60})_2\text{Co}^{\text{II}}\text{P}$ in CH_2Cl_2 .

Compound	$E_{1\text{D}_{\text{ox}}}$	$E_{2\text{D}_{\text{ox}}}$	$E_{1/2}(\text{D}^{\bullet+}/\text{D})$	$E_{1\text{A}_{\text{red}}}$	$E_{2\text{A}_{\text{red}}}$	$E_{1/2}(\text{A}/\text{A}^{\bullet-})$	$-\Delta G_{\text{CR}}, \text{eV}$	$-\Delta G_{\text{CS}}, \text{eV}$
$(\text{PyC}_{60})_2\text{Co}^{\text{II}}\text{P}$	0.80	1.17	0.74	-0.64	-1.02	-0.58	1.32	0.72

$$-\Delta G_{\text{CR}} = E_{1/2}(\text{D}^{\bullet+}/\text{D}) - E_{1/2}(\text{A}/\text{A}^{\bullet-})^{\text{a}}$$

$$-\Delta G_{\text{CS}} = E_{0-0} - (-\Delta G_{\text{CR}})^{\text{a}}$$

^a A. Bagaki, H.B. Gobeze, G. Charalambidis, A. Charisiadis, C. Stangel, V. Nikolaou, A. Stergiou, N. Tagmatarchis, F. D'Souza and A.G. Coutsolelos, *Inorg. Chem.*, 2017, **56**, 10268-10280.

$E_{1\text{D}_{\text{ox}}}$ – the first oxidation potential of electron donor ($\text{Co}^{\text{II}}\text{P}$).

$E_{2\text{D}_{\text{ox}}}$ – the second oxidation potential of electron donor.

$E_{1/2}(\text{D}^{\bullet+}/\text{D})$ – the potential for the first oxidation process of the donor.

$E_{1\text{A}_{\text{red}}}$ – the first reduction potential of electron acceptor (PyC_{60}).

$E_{2\text{A}_{\text{red}}}$ – the second reduction potential of electron acceptor.

$E_{1/2}(\text{A}/\text{A}^{\bullet-})$ – the potential for the first reduction process of the acceptor.